www.editada.org

International Journal of Combinatorial Optimization Problems and Informatics, 18(1) 2027, 14-31. ISSN: 2007-1558.
https://doi.org/10.61467/2007.1558.2027.v18i1.1481

A Digital-Twin-Oriented Virtual Prototyping Framework for Modeling, Control, and Validation of an Anthropomorphic Robotic Hand

Carlos Hernandez-Santos[1], Amadeo Hernandez[2], Arnoldo Fernandez-Ramirez[1], Roxana Garcia-Andrade[1], Nain de la Cruz[3], Armando Martinez-Reyes[1] and Francisco Fabián Tobías-Macías[4]

[1]Tecnológico Nacional de México/IT de Nuevo León, Av. Eloy Cavazos 2001, Guadalupe 66170, Nuevo León, México.
[2]Tecnológico Nacional de México/IT de Pachuca, México, Blvd. Felipe Ángeles Km. 84.5, Venta Prieta, 42083 Pachuca de Soto, Hgo.
[3]Centro de Investigación y de Estudios Avanzados del IPN, Unidad Monterrey, Vía del Conocimiento 201, Parque PIIT, Apodaca 66600, Nuevo León, Mexico.
[4] Tecnológico Nacional de México/Instituto Tecnológico de Piedras Negras.
E-mails {arnoldo.fr, roxana.ga, armando.mr}@nuevoleon.tecnm.mx, carlos.hernandez@itnl.edu.mx, nain.ca@cinvestav.mx, francisco.tm@piedrasnegras.tecnm.mx

Corresponding author: *Amadeo Hernandez,* amadeo.hh@pachuca.tecnm.mx

Abstract. This paper presents the design, mathematical modeling, control, and virtual validation of a fifteen-degree-of-freedom anthropomorphic robotic hand using a Digital-Twin-oriented virtual prototyping framework. The mechanical structure was designed in SolidWorks and integrated into MATLAB/Simscape Multibody to develop a physics-based multibody virtual prototype. Forward and inverse kinematics were formulated using the Denavit–Hartenberg convention, while the dynamic model was derived through the Euler–Lagrange formulation. A proportional-derivative controller with gravity compensation was implemented and closed-loop stability was demonstrated using Lyapunov theory and LaSalle's Invariance Principle. The analytical model was verified through Simscape Multibody simulations, showing close agreement between theoretical predictions and the virtual prototype. Simulation results demonstrated accurate joint trajectory tracking, stable convergence, and bounded actuator torque requirements throughout the prescribed motions. The proposed framework provides an effective platform for validating mechanical design and control strategies before physical implementation, establishing a validated virtual foundation for future Digital Twin integration.

Keywords: Robotic hand; Digital Twin; Simscape Multibody; PD control with gravity compensation; Virtual prototyping.

Article Info
Received: Jun 15, 2026
Accepted: Aug 01, 2026

1 Introduction

Anthropomorphic robotic hands represent one of the most challenging research topics in modern robotics because they seek to reproduce not only the morphology of the human hand but also its dexterity, adaptability, and manipulation capabilities. Their development requires the integration of multiple disciplines, including mechanical design, kinematic and dynamic modeling, control theory, sensing technologies, manufacturing processes, and intelligent algorithms. Due to the large number of interconnected mechanical components and the highly nonlinear dynamics involved, the design process has progressively shifted from conventional trial-and-error approaches toward model-based virtual development methodologies that reduce development costs and accelerate prototype validation (Gama Melo et al., 2014; Mannam et al., 2024).

Significant advances have been reported in the mechanical design of anthropomorphic robotic hands during the last decade. Research has explored rigid, tendon-driven, compliant, and soft robotic architectures to improve dexterity while reducing weight and manufacturing complexity. Tendon-driven mechanisms have demonstrated excellent grasp adaptability but often require complex transmission systems and calibration procedures (Fang et al., 2019). Soft robotic hands improve safety and adaptability during manipulation tasks; however, they generally rely on nonlinear actuator models that complicate dynamic analysis and controller design (Mohammadi et al., 2020; Perera et al., 2024). Likewise, recent co-optimization methodologies simultaneously address mechanical design and control performance, although they usually require computationally intensive optimization procedures and remain focused on specific design objectives rather than complete development workflows (Mannam et al., 2024).

Parallel to advances in mechanical design, analytical modeling has remained an essential component for robotic hand development. Forward and inverse kinematic models enable accurate motion planning and workspace analysis, while dynamic formulations provide the basis for controller synthesis and performance evaluation. Closed form inverse kinematic solutions continue to be preferred because of their computational efficiency and numerical robustness for highly articulated robotic fingers (Allahkaram et al., 2021). Similarly, the Euler–Lagrange formulation remains one of the most widely adopted methodologies for deriving nonlinear dynamic models of robotic manipulators due to its ability to explicitly represent inertial, Coriolis, centrifugal, and gravitational effects (Cheng et al., 2022; Spong et al., 2005). These analytical models provide the mathematical foundation required for implementing model-based controllers such as proportional-derivative (PD) control with gravity compensation, whose stability has been extensively studied using Lyapunov theory (Kelly, 1997; Haiyunnisa & Mahayana, 2024; Zollo et al., 2007).

Computer-aided engineering tools have also transformed the design methodology of robotic hands by enabling high-fidelity virtual prototyping before physical fabrication. CAD software packages such as SOLIDWORKS facilitate the generation of accurate three-dimensional models from which geometric dimensions, mass properties, inertia tensors, and centers of gravity can be directly extracted (Dassault Systèmes, 2024). These models can subsequently be integrated into multibody simulation environments such as Simscape Multibody, allowing simultaneous evaluation of kinematic behavior, dynamic response, actuator requirements, and control strategies within a unified simulation framework (Boschetti & Sinico, 2024; Pozzi et al., 2022). Compared with purely analytical approaches, physics-based multibody simulation considerably reduces implementation risks by validating the interaction between mechanical design and control algorithms before hardware fabrication.

Recent advances in additive manufacturing have further accelerated the development of robotic hands by enabling rapid fabrication of customized mechanical components at relatively low cost. Functional polymeric materials and three-dimensional printing technologies have demonstrated sufficient mechanical performance for robotic applications while considerably reducing manufacturing time and prototyping expenses (Shah et al., 2025). Consequently, virtual validation combined with additive manufacturing has become an increasingly attractive methodology for academic laboratories and research groups with limited development resources.

More recently, Digital Twin technology has emerged as a promising paradigm for robotic system development. A complete Digital Twin consists of a virtual representation that remains continuously synchronized with its physical counterpart through sensing, communication, and data exchange, enabling monitoring, prediction, and optimization throughout the system lifecycle (Tao et al., 2019). Before such synchronization can be achieved, however, a high-fidelity virtual prototype is required to accurately reproduce the kinematic, dynamic, and control behavior of the future physical system. Consequently, the development of reliable virtual prototypes constitutes a fundamental first step toward the realization of Digital Twin systems in robotics (Boschetti & Sinico, 2024).

Despite these important advances, several limitations remain in existing literature. Most published studies focus primarily on one aspect of robotic hand development, such as mechanical design, kinematic analysis, dynamic modeling, controller implementation, or Digital Twin technology, without integrating these components into a unified development framework. Likewise, many Digital Twin implementations emphasize real-time synchronization with existing physical systems but provide limited methodologies for validating the complete robotic design during the early development stage, before hardware fabrication. As a result, there remains a lack of comprehensive frameworks capable of combining CAD-based design, analytical modeling, multibody simulation, controller validation, and Digital-Twin-oriented development within a single engineering workflow.

To address this research gap, this paper presents a high-fidelity virtual prototyping framework conceived as the first stage toward the implementation of a Digital Twin for a fifteen-degree-of-freedom anthropomorphic robotic hand. The proposed methodology integrates CAD-based mechanical design in SOLIDWORKS, analytical kinematic and dynamic modeling, multibody simulation in Simscape Multibody, and PD control with gravity compensation into a unified virtual environment. Rather than implementing a complete Digital Twin, the proposed framework provides the virtual layer required for future integration with a physical robotic hand, embedded sensors, and bidirectional communication. Consequently, the proposed methodology enables comprehensive virtual validation of the mechanical design, dynamic behavior, and control strategy before fabrication, reducing development costs and establishing the foundation for future Digital Twin implementation.

2 Mathematical Modeling of the Anthropomorphic Robotic Hand

2.1 Mechanical design of the anthropomorphic robotic hand

The design is based on human hands in terms of ratios, range of motion, and physical length as important criteria. As shown in Fig. 1, the proposed robotic hand is composed of four articulated fingers and one thumb, it has fifteen degrees of freedom (DOF), each finger has three DOF, where the distal phalanges are sub-actuated with exception of the thumb.

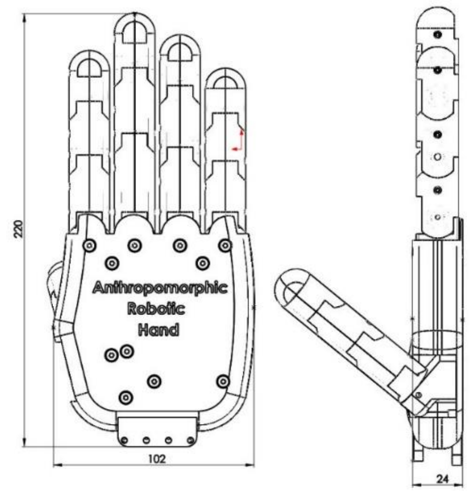

Fig. 1. Anthropomorphic robotic hand, dimension in mm

However, as shown in Table 1, some ranges of motion of the robotic hand cannot equate the human hand. The reason comes from the interference between parts of mechanical design, i.e., the 45-degree extension in a human hand cannot be achieved because the mechanical parts in the upper finger collide.

Table 1. Rate motion of anthropomorphic robotic hand

GDL	Joint		Human Hand	Robotic Hand
1	Proximal phalanx	Extension	45	-
		Flexion	90	90°
2	Middle phalanx	Extension	-	-
		Flexion	100	100
3	Distal phalanx	Extension	10	-
		Flexion	90	70

Furthermore, it is desired to design an economical robotic hand that is low cost with materials that are easily accessible and alternative from this work is use a 3D printers approach such that the fabrication of the robotic hand is fast, and the material is easy to obtain, for this work the ABS Multiple steps are required to successfully create a solid using the fused deposition technique (Crump, 1992).

2.2 CAD-Based Modeling and Virtual Prototyping Using Simscape Multibody

Simscape Multibody is a graphical modeling environment within MATLAB/Simulink that enables the modeling, simulation, and analysis of mechanical systems based on Newtonian mechanics. It employs a block-diagram approach, where interconnected components represent physical bodies and their interactions, significantly reducing modeling time and development effort (Boschetti & Sinico, 2024). The software provides extensive libraries that include rigid bodies, joints, sensors, actuators, constraints, force elements, and motion drivers. In addition to standard components, advanced blocks are available to simplify the representation and simulation of complex multibody systems. Simscape Multibody supports several analysis modes, including forward dynamics, inverse dynamics, kinematic analysis, and trimming, allowing comprehensive evaluation of mechanical behavior under different operating conditions (The MathWorks, Inc., 2024).

As an initial stage of the proposed methodology, a virtual model of the robotic hand was developed to evaluate its kinematic performance and range of motion. Figure 2 illustrates the robotic hand model implemented in Simscape Multibody. The model was generated through the integration of a three-dimensional CAD design created in SolidWorks, enabling the automatic transfer of essential physical properties such as mass distribution, inertia tensors, geometric dimensions, and coordinate system orientations into the simulation environment (The MathWorks, Inc., 2024). This integration results in a high-fidelity multibody representation capable of performing forward kinematic and dynamic analyses, providing an effective platform for validating the mechanical design and assessing the motion capabilities of the robotic hand before physical prototyping.

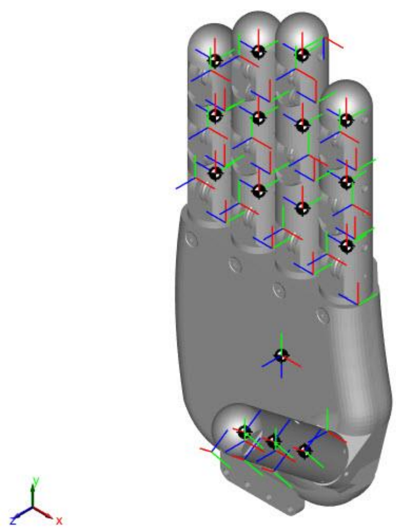

Fig 2. Model of Anthropomorphic robotic hand on Simscape.

Figure 3 presents the Simscape Multibody model of the anthropomorphic robotic hand automatically generated from the CAD assembly. The complete model is organized into six main subsystems corresponding to the anatomical structure of the hand: the thumb, index, middle, ring, and little fingers, as well as the palm. This modular architecture facilitates the analysis and control of individual finger movements while preserving the overall kinematic behaviour of the hand.

The simulation environment incorporates several fundamental blocks required for accurate dynamic modelling. The Environment (Env) block defines the gravitational acceleration vector, which in this study is oriented along the y-axis. The Root Ground block establishes a fixed reference frame by constraining one side of a joint to a stationary position within the global coordinate system, thereby providing the base support for the entire hand structure. Additionally, the Bushing block is employed to model compliant connections between components, allowing three rotational and three translational degrees of freedom. This capability enables the representation of realistic mechanical interactions, flexibility, and damping effects within the multibody system, contributing to a more accurate simulation of the robotic hand dynamics.

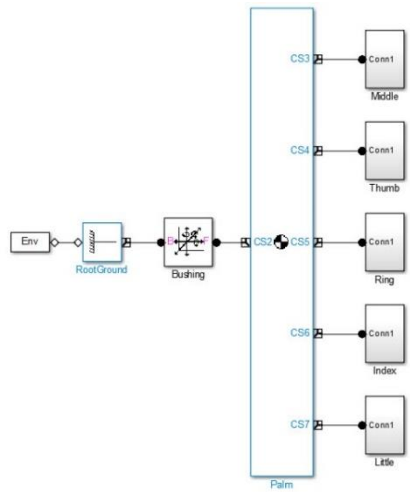

Fig. 3. Modelling of robotic hand.

The Figure 4 illustrates the Simscape Multibody model of the middle finger. The finger is composed of three rigid links connected through revolute joints, with each degree of freedom (DOF) actuated by an individual servo motor. The actuator input is defined as the applied joint torque, while the corresponding outputs include the angular position and angular velocity of each joint.

The physical parameters of the model, including link mass, inertia tensor, and center of gravity, were extracted directly from the SolidWorks CAD model and automatically incorporated into the simulation environment (Dassault Systémes, 2024). These properties are concentrated at the centroid of each link to accurately represent the dynamic behaviour of the finger during motion. The resulting model enables the evaluation of both kinematic and dynamic responses under different actuation conditions.
Since the remaining fingers share a similar mechanical architecture and joint configuration, the modelling procedure developed for the middle finger can be readily replicated to construct the complete anthropomorphic robotic hand. This modular approach simplifies the modelling process while ensuring consistency across all finger subsystems.

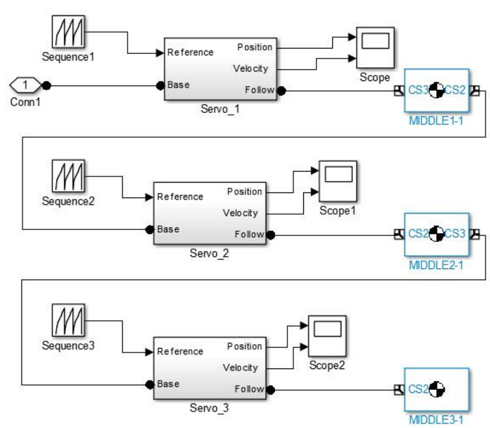

Fig. 4. Modelling of fingers.

2.3 Kinematic Analysis of the Robotic Fingers

The kinematic analysis presented in this study focuses on an individual robotic finger, as depicted in Fig. 5, Each finger is represented as a three-degree-of-freedom (3-DOF) serial manipulator composed of three rigid links L1, L2 and L3 interconnected through three revolute joints q1, q2 and q3. Reference coordinate frames are assigned to each joint following the Denavit–Hartenberg (DH) convention, allowing a systematic formulation of the forward and inverse kinematic models. The resulting mathematical representation describes the position and orientation of the fingertip and serves as the basis for workspace analysis, dynamic modeling, and control system design.

Consider the base frame (X, Y) at the joint proximal as the global reference frame. Since the general kinematic structures of all fingers of robotic hand are identical to Fig. 5, this paper assigns identical coordinate frames for the other fingers for convenience.

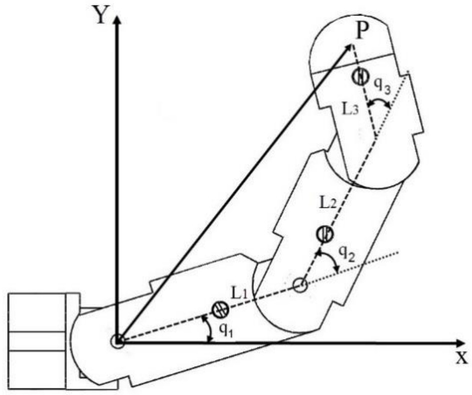

Fig. 2. Kinematic for the fingers.

The problem of kinematics is to describe the manipulator motion without consideration of the forces and torques causing the motion where the problem of forward kinematics, which is to determine the position and orientation of the end effector given the values for the joint variables of the robot [18]. The analysis of Direct Kinematics was made using the Denavit-Hartenberg (DH) convention (Denavit & Hartenberg, 1955). Table II shows the DH parameters where qi is the angle between xi-1 and xi axes as measured about zi-1 axis; di is the distance from xi-1 to xi axes as measured along zi axis; ai is the distance from zi-1 to zi axes measured along xi-1 axes; αi the angle between zi and zi-1 axes measured about xi axes. The angles are assumed positive, counterclockwise about the rotation axis.

Table 2. Finger DH parameters

DH parameters	Joint 1	2	3
q_i	q_1	q_2	q_3
d_i	0	0	0
a_i	L_1	L_2	L_3
α_i	0	0	0

The position and orientation of the distal phalanx of a finger can be obtained by the Eqs. (1) to (3).

$$p_x = L_3\left(C_1 C_{23} - S_1 S_{23}\right) + L_2 C_{12} + L_1 C_1 \quad (1)$$

$$p_y = L_3\left(S_1 C_{23} + C_1 S_{23}\right) + L_2 S_{12} + L_1 S_1 \quad (2)$$

and $$p_z = 0 \quad (3)$$

Where $S_i=sin(q_i)$, $Ci=cos(q_i)$, $S_{ij}=sin(q_i+q_j)$, and $C_{ij}=cos(q_i+q_j)$.

Once the forward kinematics is obtained, the next step is to solve the solution of inverse kinematics for the fingers, to obtain the joint q1, q2, and q3 this works uses the geometrical approach, from Fig. 5 the closed equation that model the finger is shown in Eqs. (4) to (6).

$$q_1 = \tan^{-1}\left(\frac{p_y}{p_x}\right) - \tan^{-1}\left(\frac{L_1 \sin(q_2) + L_3 \sin(2q_2)}{L_1 + L_2 \cos(q_2) + L_3 \cos(2q_2)}\right) \quad (4)$$

$$q_2 = \cos^{-1}\left(-\frac{2L_1L_2 + 2L_2L_3 \mp \sqrt{(2L_1L_2 + 2L_2L_3)^2 - 16L_1L_3\left(L_1^2 + L_2^2 + L_3^2 - p_x^2 - p_y^2 - 2L_1L_3\right)}}{8L_1L_3}\right) \quad (5)$$

and
$$q_3 = kq_2 \quad k \approx \frac{7}{11} \tag{6}$$

2.4 Digital Oriented Virtual Prototyping Framework

Digital Twin technology has emerged as a powerful paradigm for the design, monitoring, optimization, and lifecycle management of engineering systems. A complete Digital Twin consists of a virtual representation that remains continuously synchronized with its physical counterpart through real-time sensing, communication, and bidirectional data exchange. Such integration enables condition monitoring, predictive analysis, performance optimization, and intelligent decision-making throughout the system lifecycle (Tao et al., 2019).

A fundamental prerequisite for developing a Digital Twin is the creation of a high-fidelity virtual prototype capable of accurately reproducing the mechanical, kinematic, dynamic, and control behavior of the future physical system. Accordingly, this work proposes a Digital-Twin-oriented virtual prototyping framework for an anthropomorphic robotic hand. Rather than implementing a complete Digital Twin, the proposed framework establishes the virtual layer required for its future realization by integrating computer-aided design (CAD), analytical modeling, control algorithms, and multibody simulation into a unified virtual environment.

The mechanical structure of the robotic hand was designed in SOLIDWORKS and subsequently imported into Simscape Multibody, where a high-fidelity multibody model was developed. The resulting virtual prototype incorporates the geometric dimensions, mass properties, centers of gravity, and inertia tensors extracted directly from the CAD assembly, allowing realistic simulation of the robotic hand under different operating conditions.

The Figure 6 shown the proposed Digital-Twin-oriented virtual prototyping framework. The process begins with the generation of desired joint-space trajectories, which are converted into joint variables through inverse kinematic analysis. These joint variables are applied to the multibody model implemented in Simscape Multibody, where the dynamic behavior of the robotic hand is simulated. A proportional-derivative (PD) controller with gravity compensation regulates joint motion and computes the required actuation torques. The resulting joint states are processed through forward kinematics to estimate the position and orientation of the fingertip, enabling the evaluation of tracking accuracy, actuator torque requirements, workspace characteristics, and overall dynamic performance.

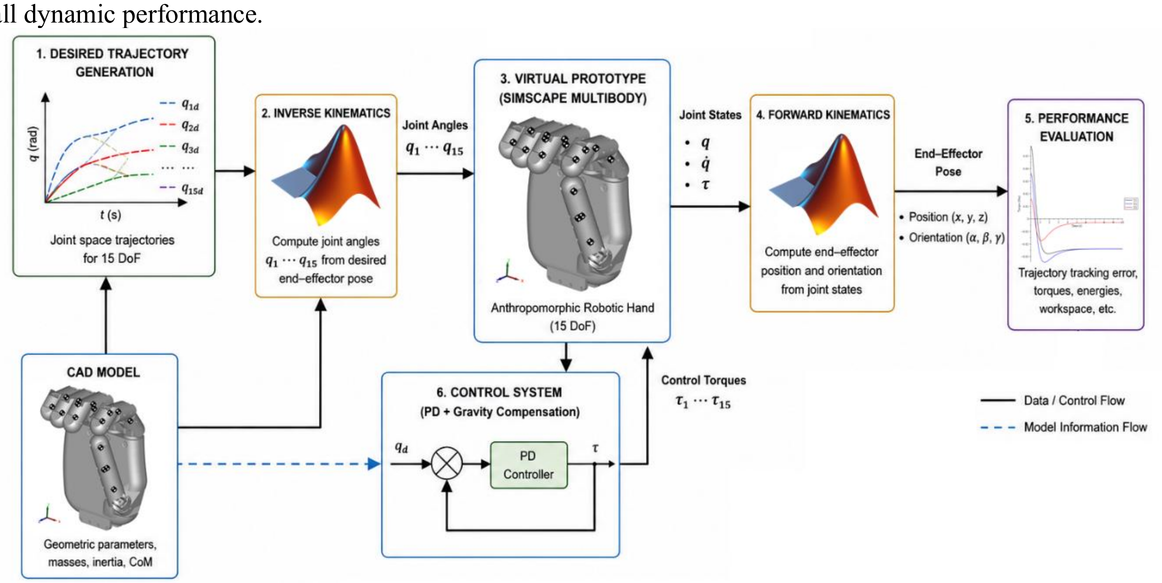

Fig. 6. Digital-Twin-oriented virtual prototyping framework integrating CAD modeling, analytical kinematic and dynamic models, multibody simulation in Simscape Multibody, and control implementation for the virtual validation of an anthropomorphic robotic hand.

The proposed framework is organized into three functional layers. The design layer includes the CAD model and the extraction of physical parameters required for simulation. The virtual layer integrates the analytical kinematic and dynamic models, the multibody representation, and the control algorithms within the Simscape Multibody environment, providing a high-fidelity virtual prototype of the robotic hand. Finally, the analysis layer performs trajectory generation, controller evaluation, and performance assessment while providing the architecture required for future integration of sensing, embedded control, and communication modules.

The present research focuses exclusively on the development and validation of this virtual prototype. Therefore, the proposed framework should be interpreted as the virtual component of a future Digital Twin, rather than as a complete Digital Twin implementation. Future work will include the fabrication of the anthropomorphic robotic hand using additive manufacturing techniques, the integration of embedded sensors and actuators, and the implementation of bidirectional communication for real-time synchronization between the physical system and its virtual counterpart.

Consequently, the proposed high-fidelity virtual prototype provides an effective platform for validating the mechanical design, kinematic behavior, dynamic response, and control strategy before physical implementation. This virtual-first methodology reduces development costs, shortens design iterations, minimizes implementation risks, and establishes the technological foundation for the future realization of a complete Digital Twin for anthropomorphic robotic hands.

2.5 Dynamic Modeling Based on the Euler–Lagrange Formulation

The dynamic behavior of the anthropomorphic robotic hand was obtained using the Euler–Lagrange formulation. This approach provides a systematic methodology for deriving the equations of motion of multi-body robotic systems while accounting for inertial, gravitational, and Coriolis effects. The resulting model serves as the basis for the development of the control strategy and the virtual validation performed within the Simscape Multibody environment, the dynamic model of a n-joint robot manipulator can be written in the Lagrangian form as:

$$M(q)\ddot{q} + C(q,\dot{q}) + G(q) = \tau \tag{7}$$

where q is the joint variable n-vector and τ is the vector of generalized forces acting on the robot manipulator. ***M(q)*** is the inertia matrix, ***C(q, q)*** are the Coriolis centripetal forces, and ***G***(q) is the gravity vector. In Eq. (7) we are not considering the friction torques that are always to be found in a real robot manipulator (Spong et al., 2005).
The analysis of the dynamic model for the three-link robotic hand was derived considering the parameters shown in Fig. 7 and their values are obtained from SolidWorks. The finger moves about only on the horizontal plane *x-y*. Each finger consists of three rigid links where l_1, l_2 and l_3 are the length of the links. The masses of the links are denoted by m_1, m_2 and m_3 respectively. The distances of the rotating axes to the centers of mass are denoted by c_1, c_2 and c_3 respectively. Finally, I_1, I_2 and I_3 denote the moments of inertia of the links. The joint positions associated with the angles q_1, q_2 and q_3 are measured between each respective link and an axis which is parallel to the *x* axis. All angles are taken to be positive counterclockwise.

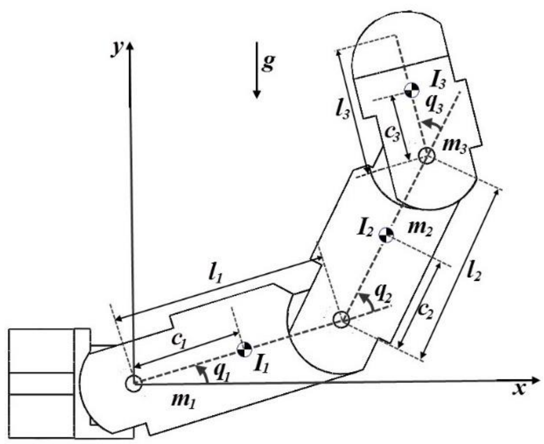

Fig. 7. Dynamic for the fingers

The approach followed in this paper applies the principles of Lagrangian dynamics, to obtain the torque in each joint of robotic hand. Recall that in the absence of friction and other disturbances, the Lagrangian $L(q,\dot{q})$ of a mechanical system is defined by

$$L(q,\dot{q}) = K(q,\dot{q}) - U(q) \tag{8}$$

Where: $K(q,\dot{q})$ y $U(q)$ represent the kinetic and potential energy of the system, respectively. Note that $q \in \Re^n$ represents the vector of generalized coordinates of the system, and $\dot{q} = \frac{d}{dt}q$ is the vector of generalized velocities. The equation of motion of Euler-Lagrange for the robotics hand given by:

$$\frac{d}{dt}\left(\frac{\partial L(q,\dot{q})}{\partial \dot{q}_i}\right) - \frac{\partial L(q,\dot{q})}{\partial q_i} = \tau_i \qquad i = 1...3 \tag{9}$$

Where $\tau_i \in \Re^n$ is the vector of external generalized forces acting on each joint of robot hand, q_i represents the position of link i, and $\dot{q}_i$ is the velocity of link i. The kinetic energy for the robotics hand is calculated by

$$K_1 = \frac{1}{2}m_1 c_1^2 \dot{q}_1^2 + \frac{1}{2}I_1 \dot{q}_1^2 \tag{10}$$

$$K_2 = \frac{1}{2}m_2\left(c_2^2\dot{q}_2^2 - 2c_2^2\dot{q}_1\dot{q}_2 - 2c_2 l_1\cos(q_2)\dot{q}_1\dot{q}_2 + c_2^2\dot{q}_1^2 + 2c_2 l_1\cos(q_2)\dot{q}_1^2 + l_1^2\dot{q}_1^2\right) + \frac{1}{2}I_2(\dot{q}_1 - \dot{q}_2)^2 \tag{11}$$

$$\begin{aligned} K_3 = \frac{1}{2}m_3 &\left(\begin{aligned} &2c_3 l_1 \dot{q}_1(\dot{q}_1 - \dot{q}_2 + \dot{q}_3)\cos(\dot{q}_2 - \dot{q}_3) + \left(2c_3 l_2\cos(q_3) + 2l_1 l_2\cos(q_2) + c_3^2 + l_1^2 + l_2^2\right)\dot{q}_1^2 \\ &+\left(\left(-4c_3 l_2\cos(q_3) - 2l_1 l_2\cos(q_2) - 2c_3^2 - 2l_2^2\right)\dot{q}_2 + 2c_3\left(c_3 + l_2\cos(q_3)\right)\dot{q}_3\right)\dot{q}_1 \\ &+\left(2c_3 l_2\cos(q_3) + c_3^2 + l_2^2\right)\dot{q}_2^2 - 2c_3\left(l_2\cos(q_3) + c_3\right)\dot{q}_2\dot{q}_3 + c_3^2\dot{q}_3^2 \end{aligned}\right) \\ &+\frac{1}{2}I_3(\dot{q}_1 - \dot{q}_2 + \dot{q}_3)^2 \end{aligned} \tag{12}$$

The potential energy for each link can be written as:

$$U_1 = -m_1 g c_1 \cos(q_1) \tag{13}$$

$$U_2 = -m_2 g l_1 \cos(q_1) - m_2 g c_2 \cos(q_1 - q_2) \tag{14}$$

$$U_3 = -m_3 g l_1 \cos(q_1) - m_3 g l_2 \cos(q_1 - q_2) - m_3 g c_3 \cos(q_1 - q_2 + q_3) \tag{15}$$

Solving the Lagrangian equations, the dynamic model of the robotic hand is:

$$\begin{aligned} \tau_1 &= m_3 l_1 c_3\cos(q_2 - q_3)(\ddot{q}_1 - \ddot{q}_2 + \ddot{q}_3) - m_3 l_1 c_3\sin(q_2 - q_3)(\dot{q}_1 - \dot{q}_2 + \dot{q}_3)(\dot{q}_2 - \dot{q}_3) + m_3 l_1 c_3\cos(q_2 - q_3)\ddot{q}_1 \\ &-m_3 l_1 c_3\sin(q_2 - q_3)(\dot{q}_2 - \dot{q}_3)\dot{q}_1 + \left[-2m_3 l_2 c_3\sin(q_3)\dot{q}_3 - 2l_1(m_2 c_2 + m_3 l_2)\sin(q_2)\dot{q}_2\right]\dot{q}_1 \\ &+\left[2m_3 l_2 c_3\cos(q_3) + 2l_1(m_2 c_2 + m_3 l_2)\cos(q_2) + m_3(l_1^2 + l_2^2 + l_3^2) + m_1 c_1^2 + m_2 l_1^2 + m_2 c_2^2 + I_1 + I_2 + I_3\right]\ddot{q}_1 \\ &+\left[2m_3 l_2 c_3\sin(q_3)\dot{q}_3 + l_1(m_2 c_2 + m_3 l_2)\sin(q_2)\dot{q}_2\right]\dot{q}_2 + \left[m_3 l_2 c_3\cos(q_3) + m_3 c_3^2 + I_3\right]\ddot{q}_3 - m_3 l_2 c_3\sin(q_3)\dot{q}_3^2 \\ &-\left[2m_3 l_2 c_3\cos(q_3) + l_1(m_2 c_2 + m_3 l_2)\cos(q_2) + m_3(l_2^2 + c_3^2) + m_2 c_2^2 + I_2 + I_3\right]\ddot{q}_2 \\ &-(m_1 c_1 - m_2 l_1 - m_3 l_1)g\sin(q_1) + (m_2 c_2 + m_3 l_2)g\sin(q_1 - q_2) + m_3 c_3 g\sin(q_1 - q_2 + q_3) \end{aligned} \tag{16}$$

$$\begin{aligned} \tau_2 &= -m_3 l_1 c_3\cos(q_2 - q_3)\ddot{q}_1 + m_3 l_1 c_3\sin(q_2 - q_3)(\dot{q}_2 - \dot{q}_3)\dot{q}_1 + \left[2m_3 l_2 c_3\sin(q_3)\dot{q}_3 + l_1(m_2 c_2 + m_3 l_2)\sin(q_2)\dot{q}_2\right]\dot{q}_1 \\ &-\left[2m_3 l_2 c_3\cos(q_3) + l_1(m_2 c_2 + m_3 l_2)\cos(q_2) + m_3(l_2^2 + c_3^2) + m_2 c_2^2 + I_2 + I_3\right]\ddot{q}_1 - 2m_3 l_2 c_3\sin(q_3)\dot{q}_2\dot{q}_3 \\ &+\left[2m_3 l_2 c_3\cos(q_3) + m_3(l_2^2 + c_3^2) + m_2 c_2^2 + I_2 + I_3\right]\ddot{q}_2 - \left[m_3 l_2 c_3\cos(q_3) + m_3 c_3^2 + I_3\right]\ddot{q}_3 + m_3 l_2 c_3\sin(q_3)\dot{q}_3^2 \\ &+l_1(m_2 c_2 + m_3 l_2)\sin(q_2)\left[\dot{q}_1^2 - \dot{q}_1\dot{q}_2\right] - (m_2 c_2 + m_3 l_2)g\sin(q_1 - q_2) + m_3 l_1 c_3\sin(q_2 - q_3)(\dot{q}_1 - \dot{q}_2 + \dot{q}_3)\dot{q}_1 \\ &-m_3 c_3 g\sin(q_1 - q_2 + q_3) \end{aligned} \tag{17}$$

$$\tau_3 = m_3 l_1 c_3 \cos(q_2 - q_3)\ddot{q}_1 - m_3 l_1 c_3 \sin(q_2 - q_3)(\dot{q}_2 - \dot{q}_3)\dot{q}_1 + \left[m_3 c_3^2 + I_3\right]\ddot{q}_3 - m_3 l_2 c_3 \sin(q_3)(\dot{q}_1 - \dot{q}_2)\dot{q}_3 + \left[m_3 l_2 c_3 \cos(q_3) + m_3 c_3^2 + I_3\right](\ddot{q}_1 - \ddot{q}_2) - m_3 c_3 \begin{Bmatrix} -g\sin(q_1 - q_2 + q_3) + \\ \left[l_1 \sin(q_2 - q_3)\dot{q}_1 - l_2 \sin(q_3)(\dot{q}_1 - \dot{q}_2)\right](\dot{q}_1 - \dot{q}_2 + \dot{q}_3) \end{Bmatrix} \quad (18)$$

Where τ_1, τ_2 and τ_3 represent the torques in the robotics hand.

3 Control Design and Stability Analysis

3.1 PD Control with Gravity Compensation

To calculate the position and torque in each joint, this paper considers a PD control law with gravity compensation (Fu et al., 1987), given by the equation:

$$\tau = K_p \tilde{q} + K_v \dot{\tilde{q}} + g(q) \quad (19)$$

Where: $K_p, K_v \in \Re^{nxn}$ represents the symmetric positive definite matrices, $\tilde{q}$ is the position error and is defined as $\tilde{q} = q_d - q$, where q_d is the desired position, and $\dot{\tilde{q}}$ is the velocity error. The control law in Eq. (19) requires information on the positions $q_d(t)$, $q(t)$ and the velocities $\dot{q}_d(t)$, and $\dot{q}(t)$ at each instant. A block diagram is present in Fig. 8 for the anthropomorphic robotic hand.
The equation that describes the closed loop behavior is obtained by combining Eqs (7) and (19) resulting in:

$$M(q)\ddot{q} + C(q,\dot{q}) + g(q) = K_p \tilde{q} + K_v \dot{\tilde{q}} + g(q) \quad (20)$$

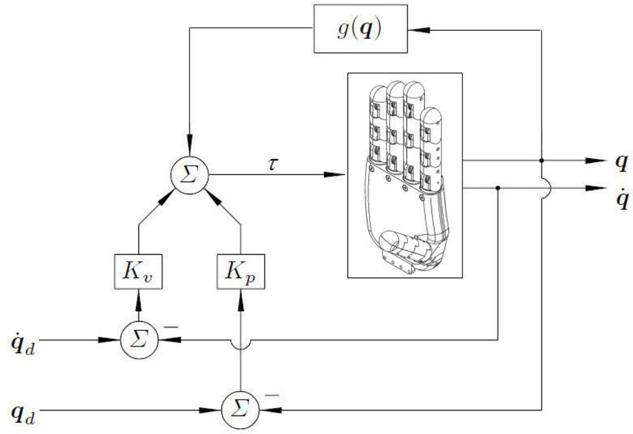

Fig. 8. PD control with gravity compensation for the Anthropomorphic robotic hand.

3.2 Stability Analysis

Theorem 1. *(LaSalle`s Invariance Principle)*

Let $f(x)$ be a locally Lipschitz function defined over a domain $D \subset \Re^n$ and $\Omega \subset D$ be a compact set that is positively invariant with respect to $\dot{x} = f(x)$. Let $V(x)$ be a continuously differentiable function defined over D such that $\dot{V}(x) \le 0$ in Ω. Let E be the set of all points in Ω where $\dot{V}(x) = 0$, and M be the largest invariant set in E. Then every solution starting in Ω approaches M as $t \to \infty$.
To apply *Theorem 1*, for stability purposes, the candidate Lyapunov function is constructed from Kinetic and Potential energies, as is presented in (Kelly, 1997) and (Haiyunnisa & Mahayana, 2024)., this with the goal to evaluate its time rate of change.

$$V(t)=\sum_{i=1}^{N}K_i+\sum_{j=1}^{M}U_j \tag{21}$$

Based on the notion that the above function is positive, which implies that is zero at the equilibrium. With the idea, to show asymptotic stability, LaSalle Theorem is applied. Since *V(t)=0* this implies that:

$$\dot{q}_1=\dot{q}_2=\dot{q}_3=0 \tag{22}$$

And therefore

$$\ddot{q}_1=\ddot{q}_2=\ddot{q}_3=0 \tag{23}$$

Applying this to the equations of motion of the system reduces to:

$$0=\left(-m_1c_1-m_2l_1-m_3l_1\right)g\sin\left(q_1\right)+\left(m_2c_2+m_3l_2\right)g\sin\left(q_1-q_2\right)+m_3c_3g\sin\left(q_1-q_2+q_3\right) \tag{24}$$

$$0=-\left(m_2c_2+m_3l_2\right)g\sin\left(q_1-q_2\right)-m_3c_3g\sin\left(q_1-q_2+q_3\right) \tag{25}$$

$$0=m_3c_3g\sin\left(q_1-q_2+q_3\right) \tag{26}$$

The Eqs. (24) to (26) show that the only solution of the system given by the last three equations which satisfies *V=0* is the equilibrium. Thus, the system is asymptotically stable.

4 Simulation Results and Discussion

4.1 Virtual Prototype Validation

The proposed anthropomorphic robotic hand was modeled using SolidWorks and simulated in the Simscape Multibody toolbox of MATLAB. This environment enables the simulation of multibody mechanical systems based on Newtonian mechanics while integrating the kinematic, dynamic, and control models within a unified framework. Numerical calculations associated with the analytical solutions of the kinematic and dynamic models were implemented using MATLAB scripts.

As described in the previous sections, the CAD model developed in SolidWorks was exported to Simscape Multibody to generate a virtual prototype of the robotic hand. This virtual environment allows the evaluation of joint mobility, dynamic behavior, and control performance prior to physical implementation. Consequently, the developed model constitutes the first stage of a Digital Twin framework for the proposed anthropomorphic robotic hand.

To verify the mobility of each joint, a repeating sequence input was applied from a reference position up to the maximum allowable range of motion defined in Table I. The simulation parameters, including mass, inertia tensors, center of gravity, and geometric dimensions, were automatically imported from the SolidWorks model, ensuring consistency between the mechanical design and the virtual prototype.

Figure 9 illustrates the motion achieved by the proximal, middle, and distal phalanges during the validation process. The obtained results confirm that the simulated joint displacements match the predefined ranges of motion specified in Table 1, demonstrating the accuracy of the virtual prototype and the correctness of the mechanical constraints implemented in the Simscape Multibody model.

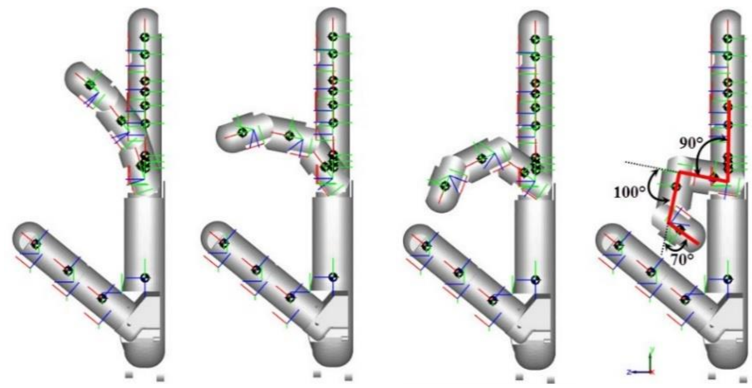

Fig. 9. Validation of the robotic finger range of motion through Simscape Multibody simulation, showing the angular displacement of the proximal, middle, and distal phalanges.

4.2 Workspace Analysis

Figure 10 present the angular displacement achieved by the proximal, middle, and distal phalanges during the mobility validation process. The simulation results obtained from Simscape Multibody closely match the predefined joint limits presented in Table I, confirming the accuracy of the mechanical constraints implemented in the virtual prototype. Furthermore, all simulation parameters, including mass properties, inertia tensors, phalange lengths, and center-of-gravity locations, were directly imported from the SolidWorks CAD model, ensuring consistency between the mechanical design and the simulation environment.To further validate the kinematic model described by Equations (1)–(3), the workspace of the robotic finger was computed and analyzed. The workspace represents the set of reachable positions of the fingertip within the allowable ranges of motion of each joint. Figure 9 presents the resulting workspace considering the geometric parameters $L_1 = 50$ mm, L_2 = 37 mm, and L_3 = 30 mm, while the joint limits were established according to the values reported in Table I.

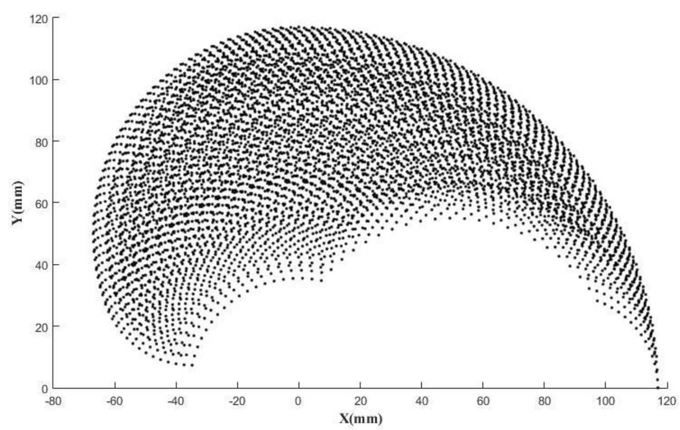

Fig. 10. Fingertip workspace generated by the forward kinematic model within the allowable ranges of motion of the three joints.

The obtained workspace demonstrates that the proposed finger mechanism can generate a broad range of motion like that of a human finger. The results also confirm the validity of the analytical forward kinematic model, since all reachable positions predicted by the mathematical formulation were successfully reproduced within the Simscape Multibody simulation environment. This agreement between the analytical and simulated results validates the proposed kinematic framework and supports its use for subsequent dynamic and control analyses.

4.3 Dynamic Response of Individual Joints

The dynamic response of the robotic finger was evaluated using the dynamic model derived from Equations (16)–(18) and the PD controller with gravity compensation presented in Section 3. The objective of these simulations was to analyze the tracking performance and the torque requirements of each joint under different reference positions. For the numerical simulations, the

parameters were obtained directly from the SolidWorks CAD model. The values used were $m_1= 0.020$ kg, $m_2= 0.020$ kg, $m_3=0.015$ kg, $l_1= 0.040$ m, $l_2= 0.035$ m, $l3= 0.023$ m, $c_1= 0.0423$ m, $c_2= 0.0798$ m, $c_3=0.1140$ m, $I_1=5.67x10^{-6}$ kg·m2, $I_2=4.2x10^{-6}$ kg·m2 , $I_3= 2.36x10^{-6}$ kg·m2, and $g=9.81$ m/s2. Also, the simulation results presented in this section were obtained using the PD controller with gravity compensation described in Section 3.1. The proportional and derivative gain matrices employed throughout all simulations were $K_p = \begin{bmatrix} 70 & 45 & 20 \end{bmatrix}$ and $K_v = \begin{bmatrix} 70 & 40 & 20 \end{bmatrix}$, these gain matrices were determined from the manipulator dynamic model derived using the Euler–Lagrange formulation. Their values were selected to satisfy the positive definiteness conditions required by the Lyapunov stability analysis, ensuring that both K_p and K_v are symmetric positive-definite matrices. Consequently, the closed-loop system satisfies the stability conditions established by LaSalle's Invariance Principle while providing accurate trajectory tracking, smooth transient response, and moderate actuator torque requirements.
Initially, the desired joint positions were established as $q_{d1}=\pi/2$, $q_{d2}=0$ and $q_{d3}=0$. Figure 11 presents the position response of joint q_1, where the desired reference is reached after approximately 6 seconds without significant oscillations or steady-state error. The corresponding control torques are shown in Figure 12. The maximum torque required by joint q_1 was approximately 0.059 Nm, while the torques generated at joints q_2 and q_3 remained within acceptable operating limits.

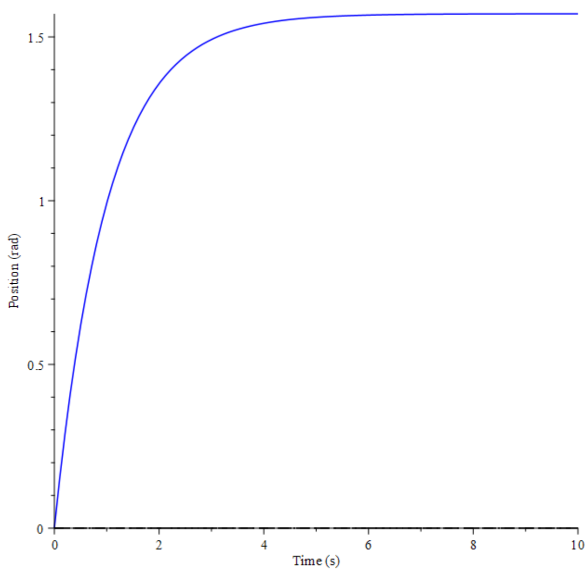

Fig. 11. Position tracking response of joint q_1 for the desired reference $q_{d1}=\pi/2$, demonstrating stable convergence and accurate trajectory tracking.

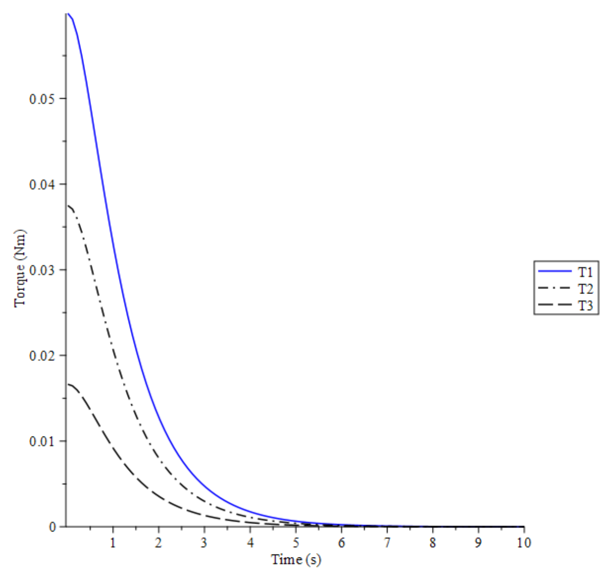

Fig. 12. Torque responses of joints q_1, q_2, and q_3 under PD control with gravity compensation for the desired position $q_{d1}=\pi/2$.

Subsequently, the dynamic behavior of the second joint was evaluated using a desired position of $q_{d2}=5\pi/9$. Figure 13 shows the position response, showing successful convergence to the reference trajectory after approximately 6 seconds. The corresponding torque profiles are presented in Figure 14, where the maximum torque generated by joint q_2 was approximately 0.037 Nm.

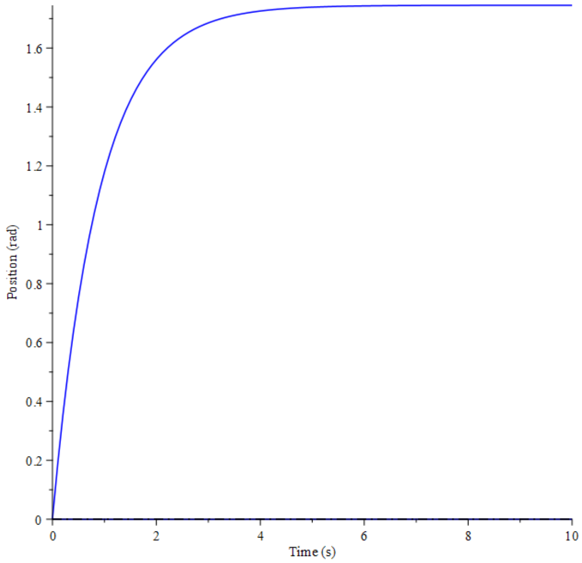

Fig. 13. Position response of joint q2 for the desired position *qd2 = 5π/9*

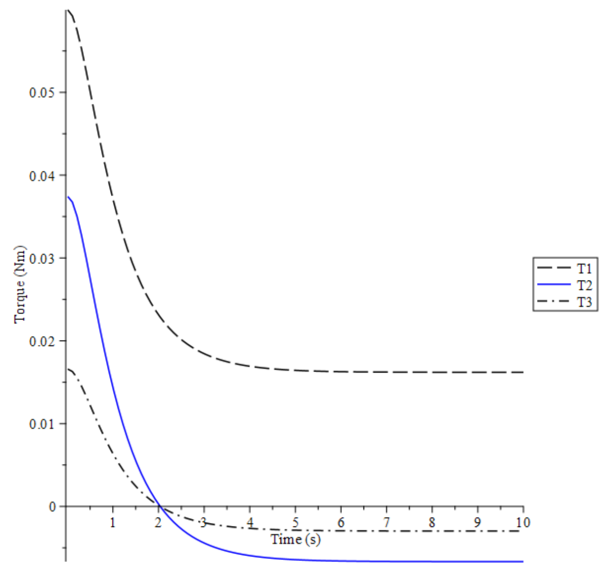

Fig. 14. Control torques generated at joints q1, q2, and q3 during the position tracking of joint q2 toward the desired reference *qd2 = 5π/9*

Finally, the third joint was analyzed considering a desired position of $q_{d3} = 7\pi/18$. The position tracking response is shown in Figure 15, while the associated torque profiles are presented in Figure 16. The simulation results indicate that the desired position was accurately achieved with a maximum torque requirement of approximately 0.018 Nm.

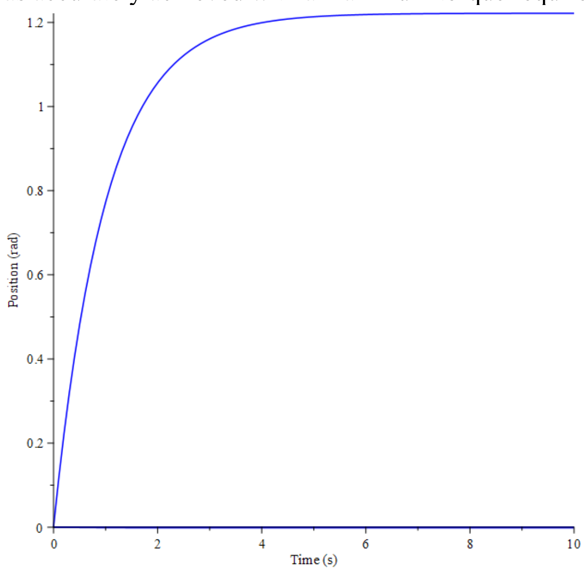

Fig. 15. Position response of joint q_3 for the desired position $q_{d3} = 7\pi/18$

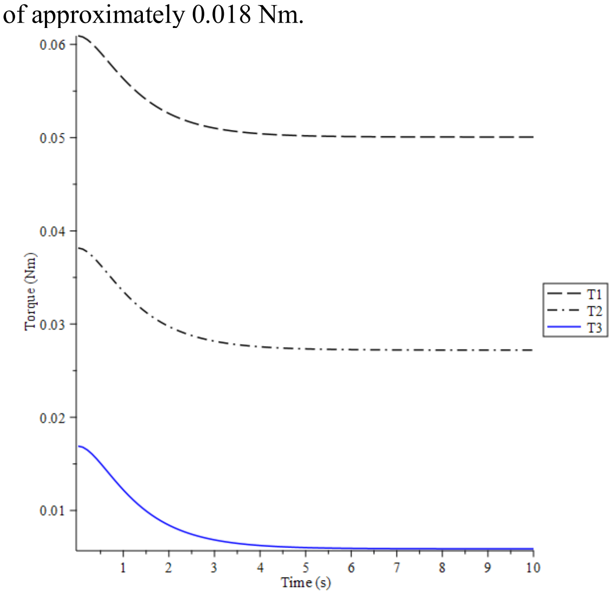

Fig. 16. Control torques generated at joints q_1, q_2 and q_3, during the position tracking of joint q_3 toward the desired reference $q_{d3} = 7\pi/18$.

Overall, the results demonstrate that the proposed control strategy provides stable and accurate trajectory tracking while maintaining low torque requirements throughout the motion range of the robotic finger.

4.4 Multi-Joint Motion Validation

To evaluate the performance of the proposed controller under simultaneous joint motion, a final simulation was conducted considering the desired positions $q_{d1} = \pi/2$, $q_{d2} = 5\pi/9$, and $q_{d3} = 7\pi/18$. This scenario represents the coordinated movement of the three phalanges and provides a more realistic assessment of the robotic finger behavior during grasping and manipulation tasks.

Figure 17 presents the position responses of the three joints. The results show that all desired trajectories were successfully achieved with stable convergence and without significant overshoot or oscillatory behavior. The settling time remained close to 6 seconds for all joints, demonstrating the effectiveness of the proposed PD controller with gravity compensation.
The corresponding torque profiles are shown in Figure 18. The maximum torques required by joints q_1, q_2, and q_3 were approximately 0.059 Nm, 0.037 Nm, and 0.018 Nm, respectively. These values are consistent with the individual joint simulations presented in the previous subsection and confirm the capability of the controller to maintain stable operation under simultaneous multi-joint actuation.

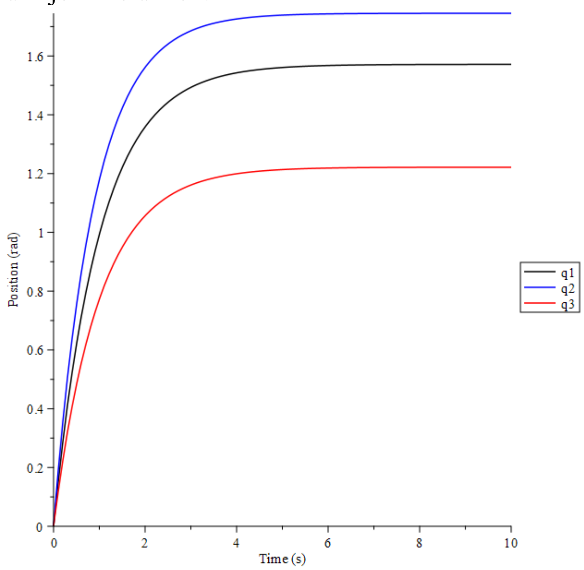

Fig. 3. Simultaneous Position Tracking of Joints q_1, q_2 and q_3.

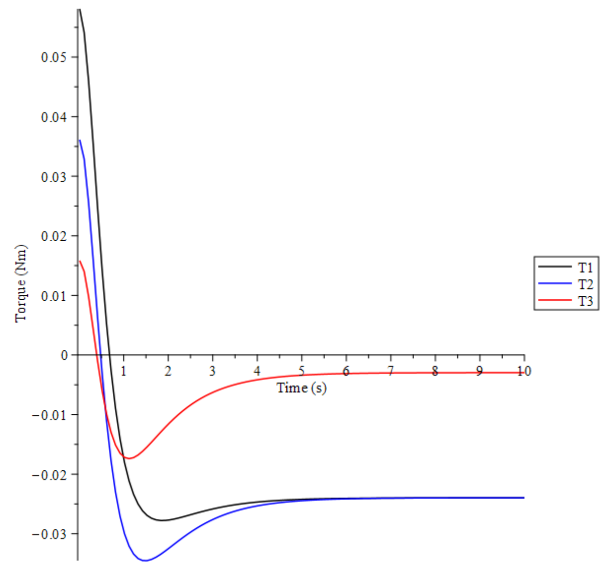

Fig. 18. Torque Profiles During Multi-Joint Motion.

Overall, the results validate the dynamic model and control strategy proposed in this work. Furthermore, the close agreement between the analytical predictions and the Simscape Multibody simulations demonstrates the suitability of the developed virtual prototype as a reliable platform for future implementation and Digital Twin integration.

4.5 Virtual Prototype Verification

The virtual prototype developed in Simscape Multibody was verified by comparing its kinematic and dynamic responses with those obtained from the analytical model derived using the Euler–Lagrange formulation. Both models were implemented using the same geometric dimensions, masses, centers of mass, and inertia tensors extracted directly from the SolidWorks CAD assembly, ensuring consistency between the analytical and multibody representations.
Figure 19 shows the complete anthropomorphic robotic hand imported into Simscape Multibody together with its multibody architecture. The CAD assembly was automatically converted into a system of rigid bodies connected by revolute joints while preserving the physical properties defined during the mechanical design stage. This virtual prototype constitutes the simulation environment used to evaluate the dynamic behavior of the robotic hand.

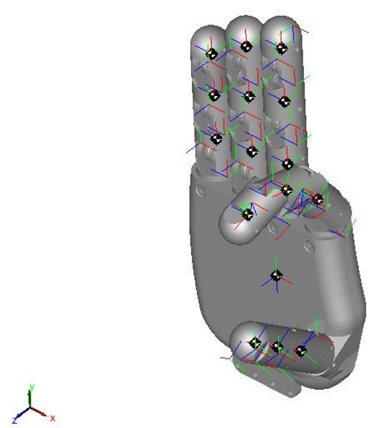

Fig. 19. CAD-based anthropomorphic robotic hand imported into Simscape Multibody

To perform the verification, identical reference joint trajectories, $q_d = \begin{bmatrix} \frac{\pi}{2} & \frac{5\pi}{9} & \frac{7\pi}{18} \end{bmatrix}^T$, were applied to both the analytical model and the Simscape Multibody model using the same PD controller with gravity compensation. The controller gains employed in both implementations were $K_p = [70 \quad 45 \quad 20]$ and $K_p = [70 \quad 40 \quad 20]$, which were selected from the dynamic manipulator to satisfy the positive-definite matrix conditions required by the Lyapunov stability analysis.
The angular responses obtained from the virtual prototype are presented in Figure 20. The three joints exhibit smooth convergence toward their desired reference positions without oscillatory behavior, reaching steady-state values consistent with those predicted by the analytical model. This agreement confirms that the forward and inverse kinematic formulations accurately reproduce the motion of the CAD-based virtual prototype.

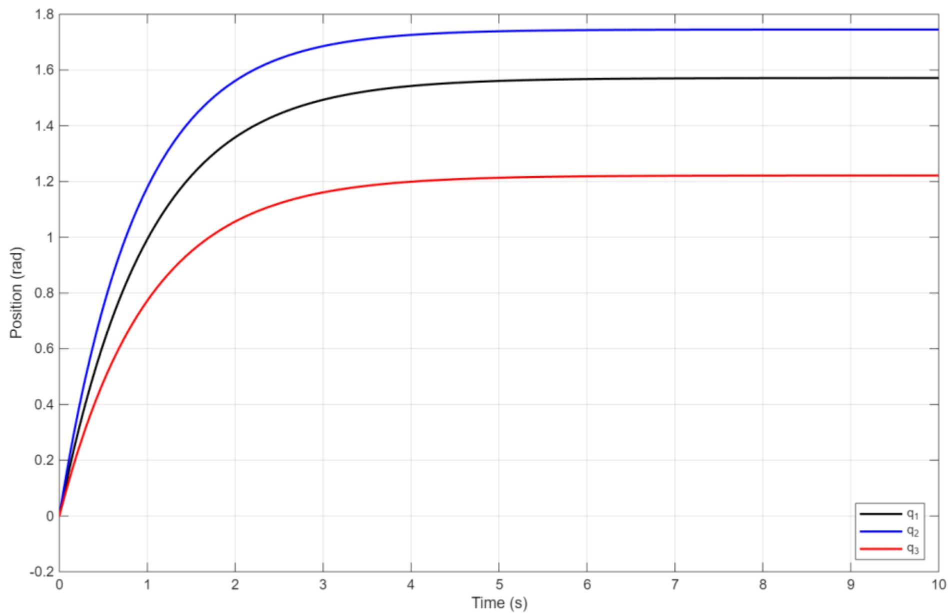

Fig. 20. Joint angular trajectories (q_1, q_2, q_3) obtained from the Simscape Multibody virtual prototype under PD control with gravity compensation.

The corresponding actuator torques are shown in Figure 21. The torque profiles present the expected transient response during the initial positioning stage, followed by convergence toward the steady-state values required to compensate for gravitational effects. The torque evolution obtained in Simscape Multibody follows the same behavior predicted by the analytical dynamic model, demonstrating consistency between both implementations.

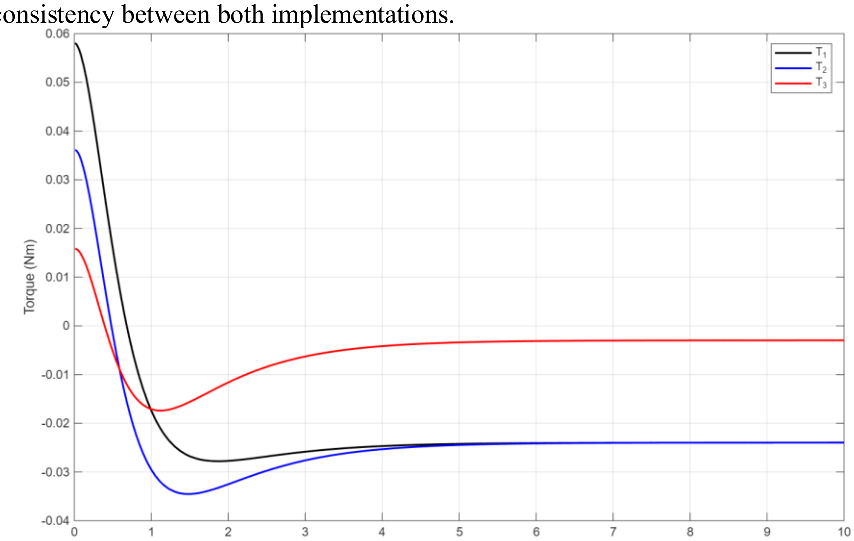

Fig. 21. Joint torque responses (T_1, T_2, T_3) obtained during the virtual validation in Simscape Multibody

Overall, the close agreement between the analytical formulation and the multibody simulation validates the proposed modeling methodology and confirms that the virtual prototype accurately reproduces the kinematic and dynamic behavior of the anthropomorphic robotic hand. Consequently, the developed virtual environment provides a reliable platform for controller evaluation, mechanical design verification, and future experimental implementation. Furthermore, although the present work is limited to virtual validation, the proposed architecture establishes the basis for a complete Digital Twin by enabling the future incorporation of real-time sensor measurements, actuator feedback, and bidirectional communication between the physical robotic hand and its virtual counterpart.

5 Conclusion

This paper presented the design, kinematic analysis, dynamic modeling, control, and virtual validation of a fifteen-degree-of-freedom anthropomorphic robotic hand through a Digital-Twin-oriented virtual prototyping framework. The proposed methodology integrates CAD-based mechanical design, analytical modeling, multibody simulation, and control techniques into a unified virtual environment for the validation of robotic hand performance prior to physical implementation.

The kinematic model was formulated using the Denavit–Hartenberg convention, allowing the derivation and validation of analytical forward and inverse kinematic solutions for the robotic fingers. Workspace analysis demonstrated that the proposed mechanism can reproduce a wide range of anthropomorphic finger motions suitable for manipulation tasks. Furthermore, the Euler–Lagrange formulation accurately described the nonlinear dynamic behavior of the system by incorporating inertial, Coriolis, centrifugal, and gravitational effects.

A proportional-derivative controller with gravity compensation was implemented to evaluate the motion performance of the robotic hand. Simulation results demonstrated accurate trajectory tracking, stable convergence, and moderate actuator torque requirements for both individual and simultaneous joint movements. Moreover, Lyapunov theory and LaSalle's Invariance Principle provided theoretical proof of the asymptotic stability of the closed-loop system, supporting the effectiveness of the proposed control strategy.

The integration of the SolidWorks CAD model, analytical kinematic and dynamic formulations, and the Simscape Multibody environment enabled the development of a high-fidelity virtual prototype capable of accurately reproducing the expected mechanical and dynamic behavior of the robotic hand. The close agreement between the analytical models and multibody simulations demonstrates that the proposed methodology provides an effective platform for validating the mechanical design, dynamic response, and control strategy before fabrication, thereby reducing development costs, shortening design iterations, and minimizing implementation risks.

Unlike a complete Digital Twin, which requires continuous synchronization with a physical counterpart through real-time sensing and bidirectional communication, the framework presented in this work focuses exclusively on the development and validation of the virtual layer required for future Digital Twin implementation. Consequently, the proposed methodology establishes a robust foundation for integrating the physical robotic hand, embedded sensors, and communication infrastructure in subsequent stages of development.

Future work will focus on manufacturing the anthropomorphic robotic hand using additive manufacturing technologies, integrating embedded sensing and actuation systems, and implementing real-time communication between the physical prototype and its virtual counterpart. These developments will enable the evolution of the proposed virtual prototype into a complete Digital Twin capable of supporting real-time monitoring, predictive maintenance, adaptive control, performance optimization, and intelligent robotic manipulation.

References

Allahkaram, M. S., Ahmadi, M. J., & Taghirad, H. D. (2021). Closed-form inverse kinematics equations of a robotic finger mechanism. In *2021 9th RSI International Conference on Robotics and Mechatronics (ICRoM)* (pp. 157–162). IEEE. https://doi.org/10.1109/ICRoM54204.2021.9663448

Boschetti, G., & Sinico, T. (2024). Designing digital twins of robots using Simscape Multibody. *Robotics, 13*(4), Article 62. https://doi.org/10.3390/robotics13040062

Cheng, J., Bi, S., Yuan, C., Cai, Y., Yao, Y., & Zhang, L. (2022). Dynamic modeling method of multibody system of 6-DOF robot based on screw theory. *Machines, 10*(7), Article 499. https://doi.org/10.3390/machines10070499

Crump, S. S. (1992). *Apparatus and method for creating three-dimensional objects* (U.S. Patent No. 5,121,329). U.S. Patent and Trademark Office. https://patents.google.com/patent/US5121329A

Dassault Systèmes. (2024). *SOLIDWORKS* (Version 2024) [Computer software]. https://www.solidworks.com/

Fang, B., Sun, F., Chen, Y., Zhu, C., Xia, Z., & Yang, Y. (2019). A tendon-driven dexterous hand design with tactile sensor array for grasping and manipulation. In *2019 IEEE International Conference on Robotics and Biomimetics (ROBIO)* (pp. 203–210). IEEE. https://doi.org/10.1109/ROBIO49542.2019.8961671

Gama Melo, E. N., Avilés Sánchez, O. F., & Amaya Hurtado, D. (2014). Anthropomorphic robotic hands: A review. *Ingeniería y Desarrollo, 32*(2), 279–313. https://doi.org/10.14482/inde.32.2.4715

Haiyunnisa, T., & Mahayana, D. (2024). Lyapunov function generation using machine learning for underactuated system. In *2024 IEEE International Conference on Smart Mechatronics (ICSMech)* (pp. 260–266). IEEE. https://doi.org/10.1109/ICSMech62936.2024.10812243

Kelly, R. (1997). PD control with desired gravity compensation of robotic manipulators: A review. *The International Journal of Robotics Research, 16*(5), 660–672. https://doi.org/10.1177/027836499701600505

Mannam, P., Liu, X., Zhao, D., Oh, J., & Pollard, N. (2024). Design and control co-optimization for automated design iteration of dexterous anthropomorphic soft robotic hands. In *2024 IEEE 7th International Conference on Soft Robotics (RoboSoft)* (pp. 332–339). IEEE. https://doi.org/10.1109/RoboSoft60065.2024.10521927

Mohammadi, A., Lavranos, J., Zhou, H., Mutlu, R., Alici, G., Tan, Y., Choong, P., & Oetomo, D. (2020). A practical 3D-printed soft robotic prosthetic hand with multi-articulating capabilities. *PLOS ONE, 15*(5), Article e0232766. https://doi.org/10.1371/journal.pone.0232766

Perera, O., Liyanapathirana, R., Gargiulo, G., & Gunawardana, U. (2024). A review of soft robotic actuators and their applications in bioengineering, with an emphasis on HASEL actuators' future potential. *Actuators, 13*(12), Article 524. https://doi.org/10.3390/act13120524

Pozzi, M., Achilli, G. M., Valigi, M. C., & Malvezzi, M. (2022). Modeling and simulation of robotic grasping in Simulink through Simscape Multibody. *Frontiers in Robotics and AI, 9*, Article 873558. https://doi.org/10.3389/frobt.2022.873558

Shah, S. K. H., Sajjad, R., Hussain, M., Anwar, M. T., Nawaz, M. S., & Raza, M. R. (2025). Additive manufacturing of functional polymers and nanocomposites for soft robotics. In C. M. Hussain & K. Deshmukh (Eds.), *Additive manufacturing of functional polymers and nanocomposites: Recent progress, applications, challenges and future opportunities* (pp. 333–350). Woodhead Publishing. https://doi.org/10.1016/B978-0-443-26516-7.00012-2

Spong, M. W., Hutchinson, S., & Vidyasagar, M. (2005). *Robot modeling and control*. John Wiley & Sons.

Tao, F., Qi, Q., Wang, L., & Nee, A. Y. C. (2019). Digital twins and cyber–physical systems toward smart manufacturing and Industry 4.0: Correlation and comparison. *Engineering, 5*(4), 653–661. https://doi.org/10.1016/j.eng.2019.01.014

The MathWorks, Inc. (2024). *Simscape Multibody* (Version R2024b) [Computer software]. https://www.mathworks.com/products/simscape-multibody.html

Zollo, L., Siciliano, B., De Luca, A., & Guglielmelli, E. (2007). PD control with on-line gravity compensation for robots with flexible links. In *2007 European Control Conference (ECC)* (pp. 4365–4370). IEEE. https://doi.org/10.23919/ECC.2007.7068344